Persistent Weakening Trend in the Spring Sensible Heat Source over the Tibetan Plateau and Its Impact on the Asian Summer Monsoon

ANMIN DUAN, FEI LI, MEIRONG WANG, AND GUOXIONG WU

State Key Laboratory of Numerical Modeling for Atmospheric Sciences and Geophysical Fluid Dynamics, Institute of Atmospheric Physics, Chinese Academy of Sciences, Beijing, China

(Manuscript received 25 January 2011, in final form 7 May 2011)

ABSTRACT

Using a dataset extended by the addition of data for 2004–08, this study reexamined the trend in the sensible heating (SH) flux at 73 meteorological stations over the Tibetan Plateau (TP) during 1980–2008 and investigated its impact on monsoon precipitation in the surrounding region. In contrast to ongoing climate warming, a weakening trend in SH is persistent over most of the plateau, despite a sharp increase in the ground–air temperature difference in 2004–08. The weakening trend in SH over the TP is primarily a response to the spatial nonuniformity of large-scale warming over the East Asian continent, which is characterized by much greater warming amplitude at mid- and high latitudes than over the tropics and subtropics. Furthermore, the suppressed air pump effect, which is driven by SH over the TP and acts as a strong forcing source, gives rise to reduced precipitation along the southern and eastern slopes of the plateau, and increased rainfall over northeastern India and the Bay of Bengal. No significantly stable correlation exists between the SH source over the TP and the overall trend or interdecadal variability in the East Asian or South Asian summer monsoon.

1. Introduction

Many previous studies have investigated the influence of the Tibetan Plateau (TP)—which acts as a huge, intense, and elevated heat source—on the onset and maintenance of the Asian summer monsoon (ASM) and the pattern of the boreal summer climate (e.g., Yeh et al. 1957; Flohn 1960; Hahn and Manabe 1975; Yanai et al. 1992; Zhao and Chen 2001; Duan and Wu 2005). In spring, the air column over the TP changes from a heat sink to a source, driven by a dominant contribution from sensible heating (SH) before the monsoon onset (e.g., Yeh and Gao 1979; Duan and Wu 2008, hereafter DW2008). The air pump driven by SH over the TP can regulate the ASM because the heating effect along the sloping surface converges the air in the lower layer from the surrounding areas with ascending air flows that penetrate the isentropic surfaces and compensate for the surface SH (Wu et al. 1997, 2007).

Along with global warming, a substantial surface and troposphere warming has been verified over the TP (e.g., Liu and Chen 2000; Zhu et al. 2001; Niu et al. 2004; Duan et al. 2006). However, the in situ SH flux has shown a significant decreasing trend since the 1980s, with the most pronounced trend occurring in spring and summer. Although latent heating shows a minor increasing trend, the springtime atmospheric heat source over the TP showed a loss in strength during 1980–2003 (DW2008).

The effect of the heat source over the TP on interannual variations in the east ASM (EASM) is well documented. For example, a clear positive correlation has been detected between the spring heating source over the TP and the subsequent summer monsoon precipitation in the valleys of the Yangtze River and Huaihe River, whereas a negative correlation exists between the spring TP heating intensity and summer rainfall in north China (e.g., Zhao and Chen 2001; Duan et al. 2005). Zhang et al. (2004) investigated decadal changes in the spring snow depth over the TP and its influence on the EASM. The results show a close relation between an interdecadal increase in snow depth over the TP during March–April and a wetter summer over the Yangtze River valley and a dryer summer over the southeast coast of China and the Indochina Peninsula. Zhu et al. (2007)

Corresponding author address: Anmin Duan, State Key Laboratory of Numerical Modeling for Atmospheric Sciences and Geophysical Fluid Dynamics, Institute of Atmospheric Physics, Chinese Academy of Sciences, P.O. Box 9804, Beijing 100029, China.
E-mail: amduan@lasg.iap.ac.cn

DOI: 10.1175/JCLI-D-11-00052.1

argued that the atmospheric heat source and winter–spring snow over the TP are strongly correlated with a shift in the decadal pattern of summer precipitation in eastern China [a typical south (flood)–north (drought) pattern]. However, Wang et al. (2007) reported that a negative correlation between the spring heat source over the eastern TP and the EASM is only found for the period before 1978; the relation has become blurred since this date. The discrepancy between the findings of these studies may be ascribed to the different sources and lengths of the datasets and the overall intrinsic limit of reliability of diabatic heating variables in National Centers for Environmental Prediction–National Center for Atmospheric Research (NCEP–NCAR) reanalysis data for the TP region. A more reliable result, obtained using a longer observational dataset, is required to clarify the possible impacts of the heat status over the TP on the long-term trend or interdecadal variability in the ASM.

The objectives of this work are to reestimate the long-term trend in the SH source over the TP and to identify the possible connection between the change in SH over the plateau and the interdecadal variability or long-term trend of the ASM. The remainder of the paper is organized as follows: The data and analysis procedures employed in this work are described briefly in section 2. Section 3 introduces the up-to-date trend of SH over the central and eastern TP (CE-TP) and over the western TP (W-TP). The connection between the SH trend over the TP and large-scale warming is investigated in section 4. The possible influence of the spring SH over the TP on interdecadal variability in the ASM is assessed in section 5. Finally, a discussion and summary are presented in section 6.

2. Data and methodology

The data used in this study include the following:

1) Regular surface meteorological observations (subjected to quality control) for the TP region are provided by the China Meteorological Administration. Variables are collected 4 times daily [0200, 0800, 1400, and 2000 local time (LT); times are 6 h earlier than UTC], including surface air temperature (T_a), ground surface temperature (T_s), and wind speed at 10 m above the surface (V_{10}). In the CE-TP, records are available for 71 stations during 1979–2008 and for 37 stations during 1960–2008, which is adequate to assess the trend in the domain. In the W-TP, data are unavailable for land surface temperature during 2004–08 at Pulan (30.28°N, 81.25°E; 3900 m above mean sea level); consequently, we calculated SH at only two stations: Shiquanhe (32.50°N, 80.08°E; 4278 m) and Gaize (32.15°N, 84.42°E; 4415 m) during the period of 1980–2008, same as the 71-station in the CE-TP.
2) The monthly-mean air temperature, geopotential height, and zonal and meridional wind speed fields are from the monthly-mean NCEP–NCAR reanalysis (Kalnay et al. 1996), the NCEP–NCAR Reanalysis 2 [NCEP/Department of Energy (DOE); Kanamitsu et al. 2002], and the Japan Meteorological Agency (JMA), which conducted the Japanese 25-yr Reanalysis (JRA-25; Onogi et al. 2007). The horizontal resolution is 2.5° × 2.5° for NCEP–NCAR and NCEP/DOE at 17 standard pressure levels. For JRA-25, the horizontal resolution is 1.25° × 1.25°, employing 23 standard pressure levels. The NCEP–NCAR reanalysis dataset is available from 1948 to the present; the NCEP/DOE and JRA-25 datasets are available from 1979 to the present. For all three datasets, we analyzed the period from December 1979 to February 2009 to obtain the seasonal mean trend in air temperature, pressure, and zonal and meridional wind speeds for the period 1980–2008 (the winter season was averaged using data from December of a given year and January–February of the following year). In terms of interdecadal variability, we utilized NCEP–NCAR reanalysis data for 1960–2008.
3) Monthly-mean precipitation data for 1980–2008 were obtained from the Global Precipitation Climatology Project version 2.1 (GPCP; Adler et al. 2003) at a resolution of 2.5° × 2.5° and from the Global Precipitation Climatology Centre (GPCC) at a resolution of 1.0° × 1.0° (Rudolf 2005). The former covers global land and ocean, whereas the latter is available only over land.

We calculated SH using the bulk aerodynamic method as follows:

$$\mathrm{SH} = C_p \rho C_{\mathrm{DH}} V_{10} (T_s - T_a), \tag{1}$$

where $C_p = 1005\ \mathrm{J\ kg^{-1}\ K^{-1}}$ is the specific heat of dry air at constant pressure; ρ is air density, which decreases exponentially with increasing elevation; C_{DH} is the drag coefficient for heat; and V_{10} is the wind speed measured at 10 m above the ground. Here, we chose $\rho = 0.8\ \mathrm{kg\ m^{-3}}$ (Yeh and Gao 1979) and $C_{\mathrm{DH}} = 4 \times 10^{-3}$ (Li et al. 1996) for the CE-TP, and $C_{\mathrm{DH}} = 4.75 \times 10^{-3}$ for the W-TP (Li et al. 2000). For a given location, the changes in ρ and C_{DH} with time are expected to be small.

A linear regression was used to calculate the linear variation trend, and the sliding t test was adopted to check for significance in interdecadal correlations and abrupt change points. Unless stated otherwise, all the reported changes are significant at the 95% confidence level.

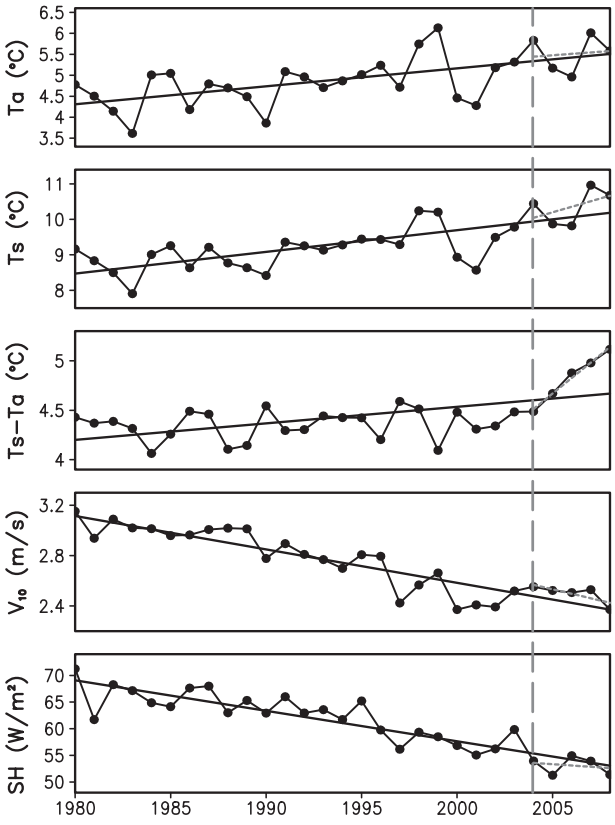

FIG. 1. Time series of the 71 station-averaged values of (top to bottom) T_a, T_s, V_{10}, and SH over the CE-TP in spring (MAM). Solid and dashed lines show the linear variation trends during 1980–2008 and 2004–08, respectively. Vertical line denotes the starting point of the 5 yr of data added to the dataset as part of the present study.

3. Up-to-date trend in the spring SH source over the TP

Figure 1 shows the time series of the 71 station-averaged values of T_a, T_s, $T_s - T_a$, V_{10}, SH, and the corresponding linear variation trend (LVT) over the CE-TP in spring [average of March–May (MAM)] for 1980–2008. Similar to the case for 1980–2003 reported by DW2008, T_a and T_s showed an increase during 2004–08, and the LVTs for T_a and T_s during the entire period (1980–2008) were 0.43 and 0.61°C decade^{-1}, respectively, which exceed the 99% confidence level (Table 1). For 2004–08, the LVT in T_s (1.6°C decade^{-1}) is much larger than that in T_a (0.33°C decade^{-1}); consequently, $(T_s - T_a)$ shows a strong increasing trend (1.6°C decade^{-1}). In contrast, the decreasing trend in V_{10} continues (-0.36 m s^{-1} decade^{-1} for 2004–08), and the corresponding LVT of 1980–2008 is significant at the 99% confidence level. According to Eq. (1), the temporal change or derivative in SH depends on the terms $(T_s - T_a)dV_{10}/dt$ and $V_{10}d(T_s - T_a)/dt$. In Fig. 1, the values of $(T_s - T_a)$ and V_{10} are positive, and the former is always larger than the latter; hence, the trend in SH depends mainly on the change in V_{10}. In other words, a declining trend in V_{10} will induce a weakening trend in SH over the TP. The LVT in spring SH over the CE-TP, as calculated in this work, was -5.7 W m^{-2} decade^{-1} during 1980–2008.

The W-TP situation is somewhat different from that of CE-TP. The warmest year of the entire period (2004) produced a slightly decreasing trend in T_a and T_s during 2004–08. Nevertheless, the decreasing trend in SH was similar to that recorded at CE-TP (Fig. 2). The SH heat source averaged over two stations in the W-TP shows a weakening trend of -5.0 W m^{-2} decade^{-1} during 1980–2008 with a relative variation rate of -10% per decade. The trends in spring T_a, T_s, $T_s - T_a$, and V_{10} are significant at the 99% level, whereas the trend in SH is below the 95% confidence level because of the relatively high mean value. In fact, the decreasing trend in SH (exceeding the 99% confidence level) occurred in all seasons over the CE-TP (Table 1). Over the W-TP, in contrast, significant change in SH was found only in summer [average of June–August (JJA)] and autumn

TABLE 1. Trend in T_a (°C decade^{-1}), T_s (°C decade^{-1}), $T_s - T_a$ (°C decade^{-1}), V_{10} (m s^{-1} decade^{-1}), and SH flux (W m^{-2} decade^{-1}) over the TP during the period 1980–2008. Significance at the 95% and 99% levels is indicated by one and two asterisks, respectively. DJF = December–February.

Region	Component	MAM	JJA	SON	DJF	Annual
CE-TP	T_a	0.43**	0.34**	0.4**	0.59**	0.44**
	T_s	0.6**	0.45**	0.52**	0.7**	0.57**
	$T_s - T_a$	0.17**	0.09	0.12**	0.15*	0.13**
	V_{10}	−0.27**	−0.2**	−0.16**	−0.19**	−0.2**
	SH	−5.73**	−4.31**	−2.52**	−2.14**	−3.675**
W-TP	T_a	0.65**	0.49**	0.6**	1.02**	0.69**
	T_s	1.17**	0.77**	0.83**	1.12**	0.97**
	$T_s - T_a$	0.56**	0.25	0.25*	0.09	0.29**
	V_{10}	−0.47**	−0.29**	−0.3**	−0.34**	0.35**
	SH	−5.0	−6.65**	−2.65*	1.52	−3.2

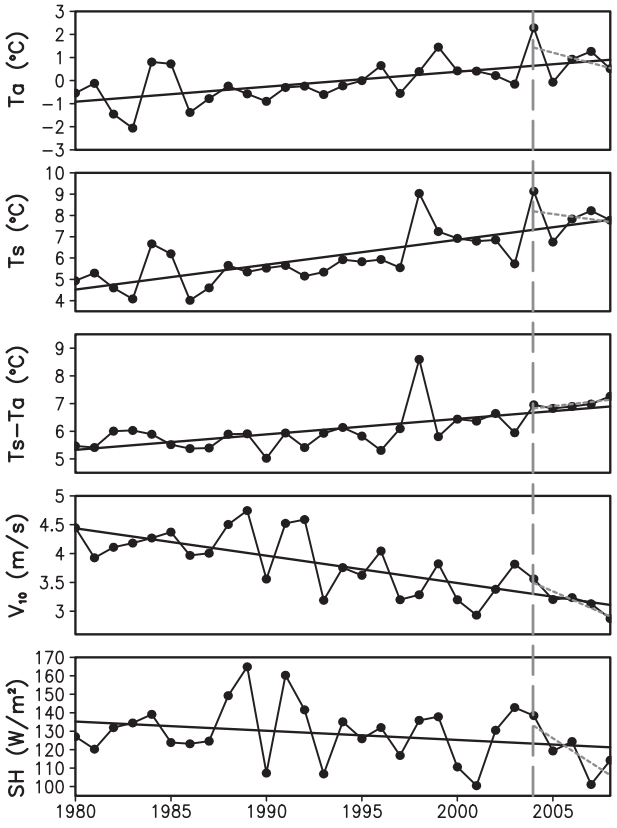

FIG. 2. As in Fig. 1, but for two station-averaged values over the W-TP in spring.

[average of September–November (SON)]. Moreover, a distinct increasing trend in SH occurred over the winter W-TP, similar to the result obtained by DW2008.

Because of the large domain considered in this analysis and the complicated topography, the trend over the TP may show spatial variations. To compare the change in terms of amplitude among various meteorological variables, Fig. 3 shows the spatial distribution of LVTs for T_a, T_s, V_{10}, and SH over the CE-TP during 1980–2008. The increasing trends in T_a and T_s, and decreasing trends in V_{10} and SH across the CE-TP are largely uniform, and a significant change in SH is seen across wide areas of the southern and middle CE-TP. In fact, for T_a, T_s, V_{10}, and SH, a significant trend (at the 95% level) is recorded by 65, 54, 59, and 46 stations, respectively (total number of stations: 71).

Generally, the trend in all variables is related to elevation, with higher elevations showing greater amplitude. In spring, this relation is seen for all variables except T_a (Table 2), but the relation is not always observed in other seasons. For example, in summer, the 29-station-averaged trend (elevations: 3000–4000 m) is positive in T_a but negative in V_{10} and SH; the opposite is observed for stations at altitudes less than 3000 m and higher than 4000 m (results not shown).

4. Relation between the change in SH and nonuniform large-scale warming

The mean altitude of the TP is about 600 hPa, and the surface flow is controlled mainly by the midtropospheric East Asian subtropical westerly jet (EASWJ). Duan and Wu (2009) reported that the trend in surface wind and the associated SH over the plateau is related to changes in the EASWJ. To demonstrate that this result is not dependent on the data source, Fig. 4 shows the temporal evolution and corresponding LVT of the spring EASWJ index, defined as the average 500-hPa zonal wind speed within the area (25°–45°N, 70°–120°E, as shown in the top-left panel of Fig. 5) over the period 1980–2008. A consistent decreasing trend in the EASWJ index is evident among all three reanalysis datasets, with the LVT significant at the 90% confidence level for NCEP–NCAR data (-0.27 m s^{-1} decade^{-1}) and at the 95% level for NCEP/DOE and JRA-25 data (-0.31 and -0.39 m s^{-1} decade^{-1}, respectively).

The geostrophic balance relation suggests that such a large-scale change in zonal wind speed can be attributed to a reduction in the in situ meridional pressure gradient. Figure 5 shows the spatial distribution of LVT in 500-hPa air temperature, geopotential height, zonal wind speed, and meridional wind speed in spring during 1980–2008. A substantial warming trend of 0.2°C –0.4°C decade^{-1} is found north of the TP, with the center near Baikal. A much weaker warming signal, or even cooling signal, is found in subtropical Asia. The Intergovernmental Panel on Climate Change Fourth Assessment Report (IPCC AR4) (Solomon et al. 2007) also reported a larger warming over the midlatitudes than over the tropics and subtropics, for both the surface and the troposphere during 1979–2005. As a result of temperature changes, geopotential height rose in warming areas and dropped in cooling areas, leading to a further weakening of the meridional pressure gradient and subsequently a weakening of the zonal wind to the south of the warming center, as required by the geostrophic balance relation (Holton 1992). Consequently, a decelerated zonal wind, with a trend exceeding -0.2 m s^{-1} decade^{-1}, appeared over and to the south of the TP. It is noteworthy that decelerated zonal winds in the western part of the TP are larger than other places, which leads to divergence over the TP. Similarly, a diminished zonal pressure gradient over subtropical East Asia, which was induced mainly by the cooling signal over the northwest Pacific, might be responsible for the decelerated meridional wind speed. Over east and south China, we obtained a negative trend in the meridional wind speed of -0.2 to -0.6 m s^{-1} decade^{-1}.

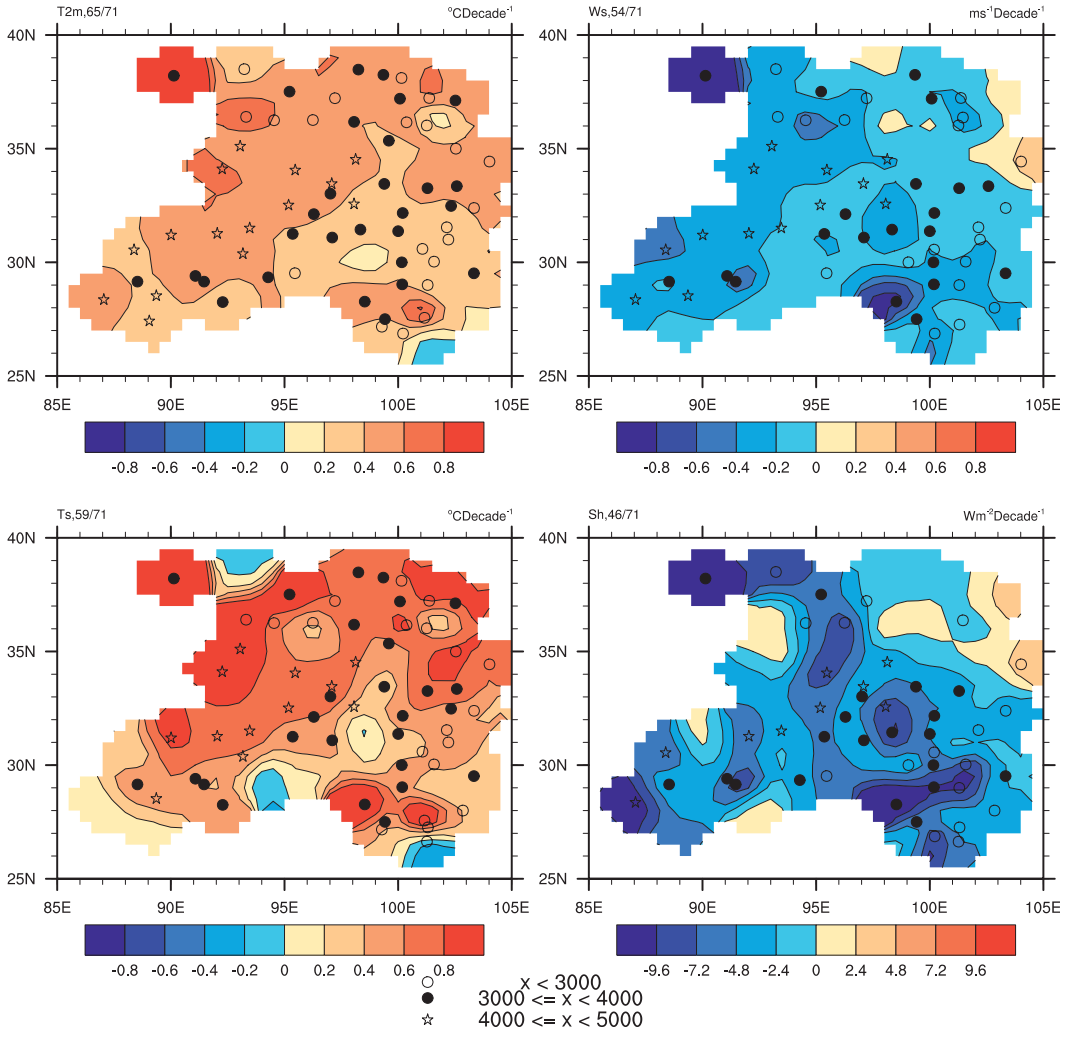

FIG. 3. Spatial distribution of the LVT in the annual mean T_a (°C decade^{-1}), T_s (°C decade^{-1}), V_{10} (m s^{-1} decade^{-1}), and SH flux (W m^{-2} decade^{-1}) over the CE-TP during the period 1980–2008. Stations with LVT significant at the 95% level are shown in each panel (the number of stations is listed at top left). Open dots, solid dots, and stars denote stations located at altitudes below 3000, at 3000–4000, and at 4000–5000 m above mean sea level, respectively.

Similar results can be found at 850 hPa, indicating a declining trend in the low-level southwesterlies.

In summer, the large-scale trends of temperature and circulation at subtropical and higher latitudes are similar to those in spring. In the tropics, an intensified zonal wind speed is found south of the TP at 500 hPa (figure not shown). Therefore, the spatially nonuniform large-scale warming, which is characterized by a stronger trend over mid and high-latitude land areas than over tropical and subtropical oceans, resulted in a diminishing trend in zonal and meridional wind speeds over the tropical and subtropical East Asian continent. In other words, the northward penetration of the southerlies over East Asia, which serve as the major supplier of moisture in the EASM, has declined in recent decades.

5. Feedback of change in SH over the TP on the ASM

a. *Precipitation trend in the ASM region*

As a response to nonuniform large-scale climate warming, will the change in SH over the TP influence the long-term trend or interdecadal variability in the ASM and the corresponding precipitation pattern or intensity? To answer this question, we now consider precipitation change in the ASM region during spring and summer, and compare the temporal evolution of the SH index over the TP with summer monsoon indices over East Asia and South Asia.

The distinctive topography and orography of East Asia produce unique features in the EASM, which comprises both tropical and subtropical subsystems. The

TABLE 2. Trend in spring (MAM) T_a (°C decade^{-1}), T_s (°C decade^{-1}), V_{10} (m s^{-1} decade^{-1}), and SH flux (W m^{-2} decade^{-1}) at 71 stations over the CE-TP during the period 1980–2008, classified by height. The term $2000 < H < 3000$ indicates heights between 2000 and 3000 m above mean sea level; $3000 < H < 4000$ indicates heights between 3000 and 4000 m; and $H > 4000$ indicates heights above 4000 m.

Region	Component	$2000 < H < 3000$ (27 stations)	$3000 < H < 4000$ (29 stations)	$H > 4000$ (15 stations)
CE-TP	T_a	0.382	0.472	0.425
	T_s	0.527	0.642	0.667
	V_{10}	−0.242	−0.250	−0.340
	SH	−5.339	−6.023	−6.199

monsoon circulation system over East Asia has a high degree of independence and differs from that over South Asia, although they are related at times (e.g., Tao and Chen 1987; Ding 1994; Lau et al. 2000). The South Asian or Indian summer monsoon is purely a tropical monsoon system. The outbreak of the tropical ASM onset consists of three successive stages: the monsoon onset over the east coast of the Bay of Bengal (BOB) in early May, the monsoon onset over the South China Sea by 20 May, and the onset of the South Asian summer monsoon (SASM) over India by 10 June. Moreover, the onset of the monsoon is directly linked to the thermal and mechanical forcing of the TP (Wu and Zhang 1998). The low-layer isentropic surfaces descend sharply and intersect the steep ground surface along the southern and eastern slopes of the plateau. Hence, the SH over the plateau, especially along the high Himalayas, operates as an efficient air pump that results in the convergence of airflow in lower layers toward the plateau. Strong negative vorticity is then created because of surface friction, forcing upper-layer anticyclonic circulation above the lower-layer cyclonic circulation (Wu et al. 1997, 2007).

Because the SH-driven air pump works mainly in spring and summer, and the magnitude of the decrease in SH during these two seasons is much larger than that during autumn and winter (Table 1), in Fig. 6 we show the spatial distribution of LVT in precipitation during 1980–2008 for spring (left) and summer (right), as calculated from two independent precipitation datasets. A significant decreasing trend is seen along the southern slope of the TP in both seasons (the LVT in spring and summer are above −0.4 and −1.0 mm day^{-1} decade^{-1}, respectively) and along the eastern slope in summer, where the topography rises sharply from 1500 to above 3000 m. The air pump effect driven by the SH over the plateau is most efficient along the south slope of the Himalayas due to the steep topography. Therefore, the weakening trend in the SH over the plateau contributed to the decreasing trend in the precipitation along its south slope at least to a certain degree.

Accompanying the substantial decreasing trend observed at the margins of the plateau, a significant increasing trend is seen for north India, BOB, and the Indochina Peninsula. Over the Indian continent, we observe a decreasing trend along the southwest coastal regions and over north India, and an increasing trend in central and northeastern India. These spatial variations obscure the average trend for India as a whole. Despite the overall similarity between those two precipitation datasets, some differences are observed in East Asia. For example, in spring, a remarkable decreasing precipitation trend appears in southeastern China in GPCC, whereas a weak increasing trend appears in GPCP. Nevertheless,

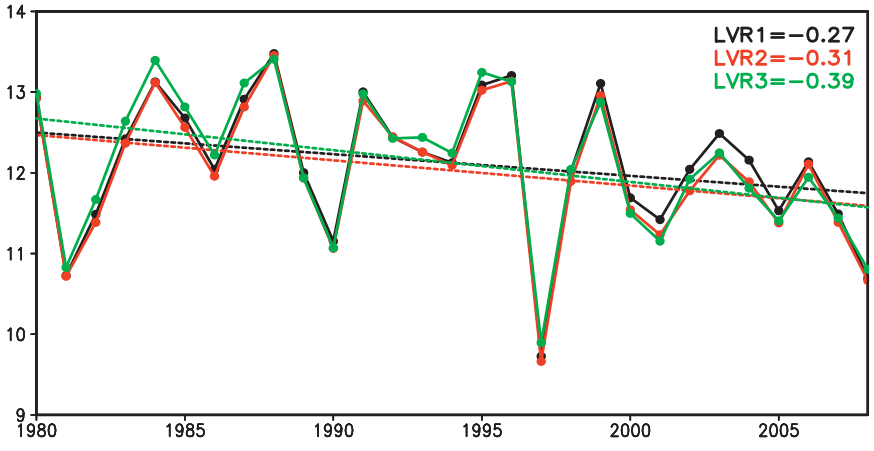

FIG. 4. Temporal evolution (solid curves) and LVT (dashed lines) of the 500-hPa EASWJ index during 1980–2008. Units for EASWJ and its LVT are m s^{-1} and m s^{-1} decade^{-1}, respectively. Black, red, and green lines represent NCEP–NCAR, NCEP/DOE, and JRA-25 data, respectively.

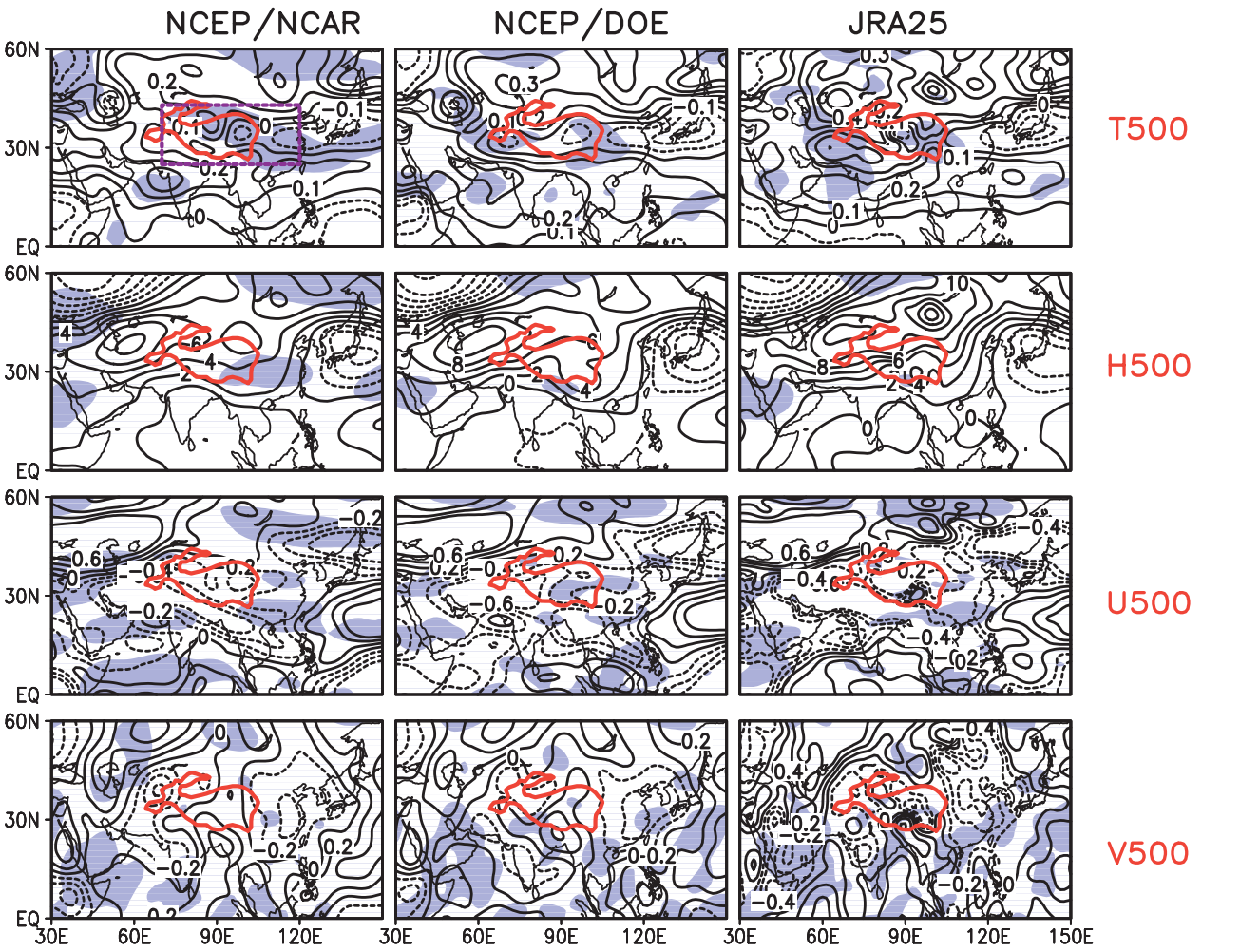

FIG. 5. Spatial distribution of LVR for (top) air temperature (°C decade^{-1}), (top middle) geopotential height (gpm decade^{-1}), (lower middle) zonal wind speed (m s^{-1} decade^{-1}), and (bottom) meridional wind speed (m s^{-1} decade^{-1}) at 500 hPa in spring (MAM) during 1980–2008. (left–right) Columns show NCEP–NCAR, NCEP/DOE, and JRA-25 data. Shaded areas denote a significant trend at the 95% level. Solid thick curves and dashed rectangle in the top-left panel denote the TP area with height above 2500 m MSL and the EASWJ domain (25°–45°N, 70°–120°E), respectively.

both datasets yield a decreasing (increasing) trend in summer rainfall in north China (south China), which has become known as the weakened EASM in recent decades (Huang et al. 2006). In China, the change in GPCC precipitation data seems to be more consistent with station-observed results (e.g., Fig. 4b in Zhou et al. 2009).

Variations in precipitation are directly related to the transportation of moisture. Figure 7 shows the climatology together with the trend in the air-column-integrated moisture-flux vector over the ASM and surrounding regions. In the climate mean field, vigorous northward moisture transportation occurs in both spring and summer over the southern slope of the TP, while it occurs only in summer over the eastern slope. During 1980–2008, the inward humid airflows are significantly suppressed along the southern and eastern slopes of the plateau, giving rise to a decreasing trend in precipitation in these regions. Over South China and the northern South China Sea, a westerly anomaly in spring (against the climate mean easterly) is indicative of the suppressed moisture supply and the corresponding decreasing trend in precipitation. Over East China, however, a northerly anomaly in summer (against the climate mean southerly) is responsible for the southward retreat of the summer monsoon rain belt. Similar results were obtained using NCEP/DOE and JRA-25 data. Thereby, the weakened air-pumping effect driven by the SH over the TP, which serves as a strong, local forcing source, plays an important role in modulating the changes in circulation and precipitation in the surrounding regions.

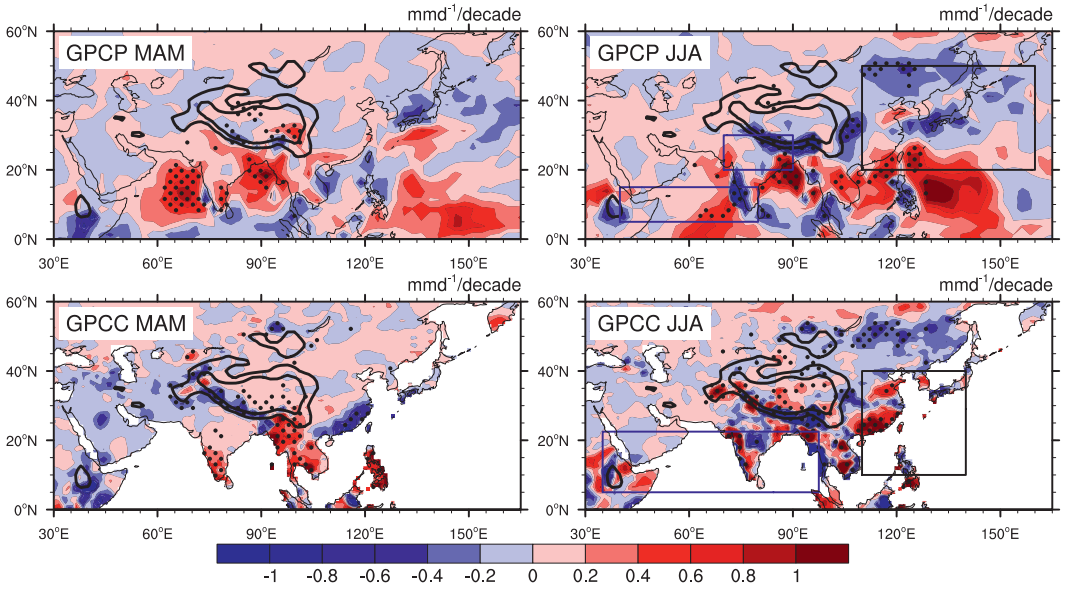

FIG. 6. Spatial distribution of the LVT in (left) spring and (right) summer precipitation during 1980–2008, for (top) GPCP data and (bottom) GPCC data; units: mm day^{-1} decade^{-1}. Dotted areas denote a significant trend at the 95% level; thick curves represent 1500 and 3000 m above mean sea level. Blue and black rectangles in the top-right panel represent the regions of the SASM and EASM indices defined by Wang and Fan (1999) and Guo (1983), respectively. Blue and black rectangles in the bottom-right panel denote the regions of the SASM and EASM indices, respectively, defined by Li and Zeng (2002).

b. *Relation between the change in SH over the TP and interdecadal variability in the ASM*

The above-mentioned results reveal the long-term trend of the SH over the TP and its influence on precipitation in the surrounding regions during recent decades. Here, we investigate whether a direct connection exists between the heat status over the TP and the overall intensity of the EASM and/or SASM in terms of the long-term trend or interdecadal variability. The best method to use to define the strength of the EASM remains a topic of controversy, in terms of the precipitation pattern and interannual variations, although various tropical ASM indices show a strong correlation with each other (Wang and Fan 1999). In this work, we chose the widely used EASM indices proposed by Guo (1983) and Li and Zeng (2002). The former is defined by the summation of the sea level pressure (SLP) gradient between land (110°E) and sea (160°E) from 10° to 50°N, and the later is a dynamically normalized seasonality. The two SASM indices are from Wang and Fan (1999) and Li and Zeng (2002). All the indices are calculated using JJA mean NCEP–NCAR reanalysis data, because both the NCER/DOE and JRA-25 reanalysis datasets are only available since 1979.

Figure 8 shows the 5-yr running mean time series of the SH index averaged for 37 stations over the TP in spring and summer (which agrees well with the 71-station-averaged result documented by DW2008), together with two EASM and two SASM indices for 1960–2008. Using the sliding *t* test, we found a significant shift point, from an increasing trend to a decreasing trend, in the SH over the TP in 1978; the decreasing trend accelerates after the mid-1980s. However, the EASM index shows a significant decrease since the mid-1970s and an increase after the 1990s, characterized by multiscale variations rather than a regularly trend. Kwon et al. (2007) reported that the EASM showed a decadal change in the mid-1990s. In other words, after the mid-1990s, a significant decrease occurred in the strength of zonal winds near the subtropical jet over East Asia, as well as a distinct increase in precipitation over southeast China. The two SASM indices show no abrupt changes during the entire period, although a weak increasing trend is seen after the 1970s.

Figure 9 shows 11-yr running correlations between the spring SH index over the TP and the EASM and SASM indices, representing their linkages in terms of interdecadal variability. The relation between the spring SH index over the TP and EASM or SASM indices shows a remarkable decadal variation. During the 1970s and 1990s, a positive correlation is seen between the spring SH over the TP and Wang and Fan's (1999) SASM index, whereas a negative correlation is observed in the 1980s. In fact, a stable negative correlation during the entire period is seen only between the spring SH over the TP and Li and Zeng's (2002) EASM index, although the relation is not significant at the 95% level for most of the period.

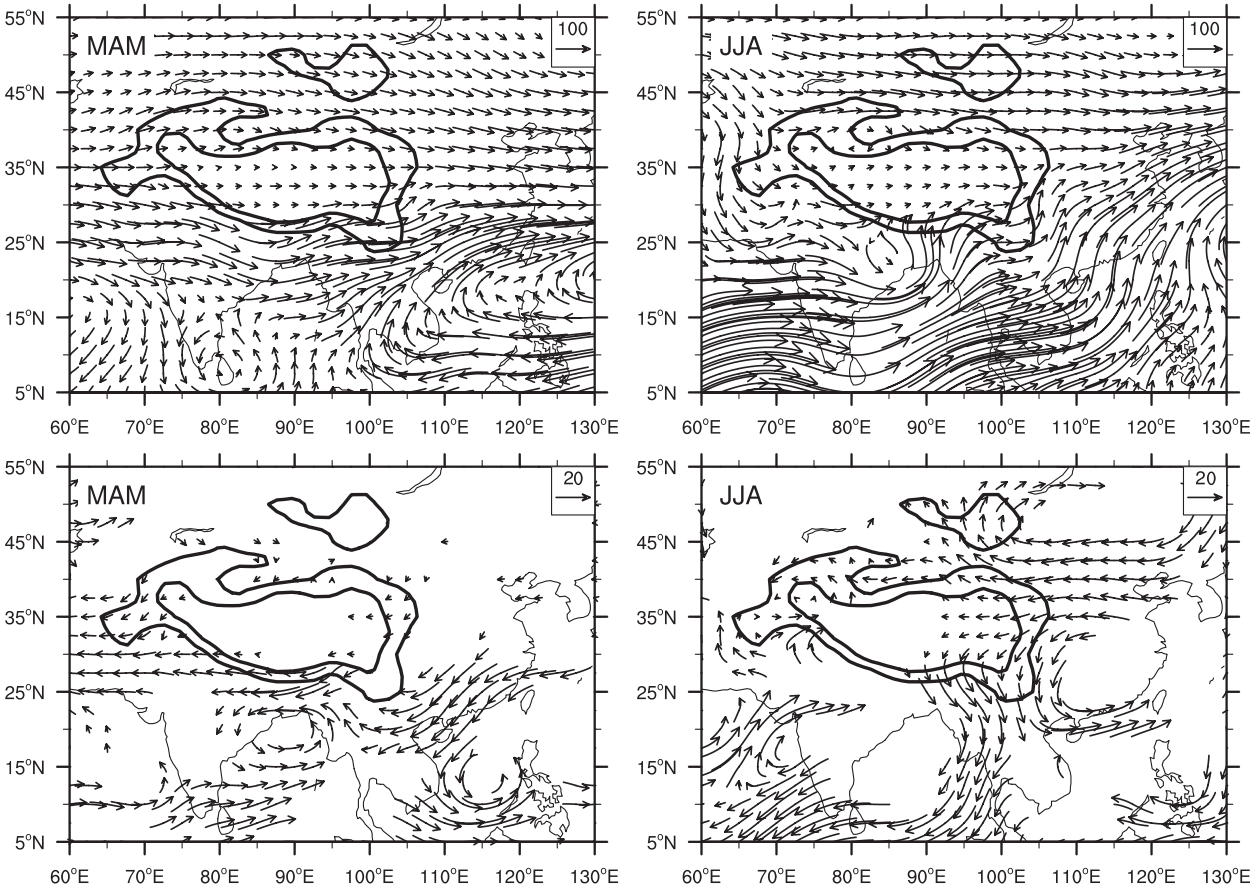

FIG. 7. (top) Climate mean (unit: kg m^{-1} s^{-1}) and (bottom) trend (unit: kg m^{-1} s^{-1} decade^{-1}) in the air-column-integrated vapor flux vector over East Asia in (left) spring and (right) summer during 1980–2008. Trends in the zonal vapor flux (uq) and meridional vapor flux (vq) only with statistical significance above 95% level are plotted.

The monsoon is considered to be an inevitable consequence of the land–sea thermal contrast; hence, a change in heat status over either land or sea may lead to a shift in monsoon intensity. Signals from the TP can partially affect the variations in EASM or SASM; however, for the overall case in ASM systems, other factors related to heat status and moisture supply (e.g., ocean conditions) may be more important in terms of regulating the long-term or interdecadal trend in the ASM. Moreover, monsoon indices typically represent the intensity of monsoon circulation for a large domain, whereas the pattern of precipitation in monsoon regions is known to be complex. Thus, it is not surprising that no stable or significant connection exists between the heat status over the TP and the ASM indices over an interdecadal time scale.

6. Summary and discussion

Using historic records from 73 meteorological stations over the TP, three reanalysis datasets, and two precipitation datasets, we reexamined the SH trend over the TP during recent decades and investigated its connection with large-scale climate warming and feedbacks to interdecadal variability in the ASM. The main findings are summarized below.

1) In contrast to substantial climate warming, a statistically significant decreasing trend in SH over the CE-TP remains ongoing. The linear trend of 71-station-averaged SH in spring during 1980–2008 is −5.7 W m^{-2} decade^{-1}. Meanwhile, the in situ ground–air temperature difference shows an accelerated increasing trend in 2004–08. A weakening trend in spring SH also occurs at two stations over the W-TP, yielding a linear trend of −5.0 W m^{-2} decade^{-1}.
2) The decreasing trend in SH over the TP is induced mainly by a reduction in surface wind speed. A much larger warming amplitude at mid- and high latitudes, compared with over the tropics and subtropics, gives rise to a decreasing trend in the meridional pressure gradient and consequently a slowing of the westerly jet over the tropical and subtropical Asian continent, as

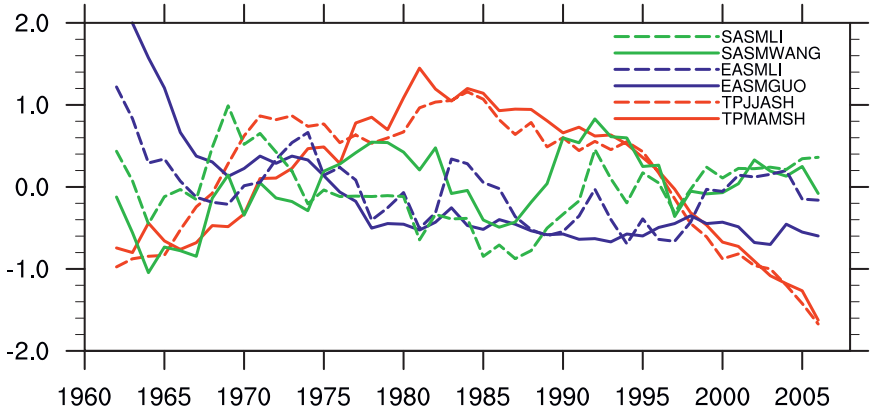

FIG. 8. Normalized time series of the 5-yr running mean of the SH index over the TP (solid red and dashed red curves represent spring and summer, respectively), two EASM indices [solid blue and dashed blue curves indicate the indexes proposed by Guo (1983) and by Li and Zeng (2002), respectively], and two South SASM indices [solid green and dashed green curves indicate the indexes proposed by Wang and Fan (1999) and by Li and Zeng (2002), respectively] during 1960–2008.

required by the geostrophic balance relation. Therefore, the weakening trend in spring SH over the TP can be regarded as a response to spatial nonuniformity in large-scale warming over Eurasia.

3) Serving as a strong forcing source, the weakened SH source over the TP in turn contributes to reduced monsoon precipitation over the southern and eastern slopes of the plateau, and to increased precipitation over northeast India, Bangladeshi, and BOB. However, variations in the EASM and SASM indices, which represent the overall circulation intensity for a large domain, show a clear multiscale variability, rather than a persistent trend, after the 1980s. There is no stable and significant correlation between the spring SH index over the TP and EASM or SASM indices in an interdecadal time scale.

Some issues still remain unresolved. For example, why does the ground–air temperature difference show a strongly increasing trend in the CE-TP during 2004–08? How can the contribution of the change in local forcing (e.g., heat status over the TP) be distinguished from that of a global atmospheric circulation shift due to the greenhouse effect? Zhou et al. (2009) reviewed the factors that may contribute to the interdecadal transition in EASM, including tropical ocean warming, change in heat status over the TP, aerosol forcing, and internal variability of the climate system. Both observational results and

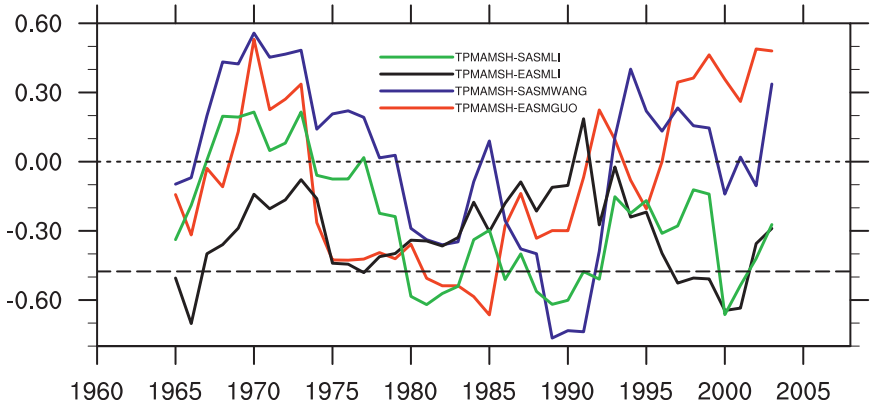

FIG. 9. Eleven-year running correlation coefficients between the spring SH over the TP and Guo's (1983) EASM index (red), Li and Zeng's (2002) EASM index (black), Wang and Fan's (1999) SASM index (blue), and Li and Zeng's (2002) SASM index (green). Dotted and dashed lines represent the zero value and 95% confidence level, respectively.

numerical experiments suggest that changes in sea surface temperature and convective activity over the tropical Indian Ocean and far western Pacific are responsible for the decadal westward extension of the western Pacific subtropical high and reduced water vapor supplied to north China from the South China Sea and from the western North Pacific since 1970s (Hu 1997; Gong and Ho 2002). However, the causes of EASM weakening remain elusive. This topic requires further investigation, particularly in terms of understanding the mechanism of the impact of heat source change over the TP on the ASM at a decadal time scale.

Acknowledgments. This work was supported jointly by the Chinese Ministry of Science and Technology (Grants 2010CB951703 and 2009CB421403), the Chinese Academy of Sciences (Grant KZCX2-YW-Q11-01-02), and the National Natural Science Foundation of China (Grant 40930530). We thank the National Oceanic and Atmospheric Administration (NOAA) of the United States for providing GPCC precipitation data.

REFERENCES

Adler, R. F., and Coauthors, 2003: The Version-2 Global Precipitation Climatology Project (GPCP) monthly precipitation analysis (1979–present). *J. Hydrometeor.,* **4,** 1147–1167.

Ding, Y., 1994: The summer monsoon in East Asia. *Monsoons over China,* Y. Ding, Ed., Atmospheric Sciences Library, Vol. 16, Kluwer Academic Publishers, 1–90.

Duan, A., and G. Wu, 2005: Role of the Tibetan Plateau thermal forcing in the summer climate patterns over subtropical Asia. *Climate Dyn.,* **24,** 793–807, doi:10.1007/s00382-004-0488-8.

——, and ——, 2008: Weakening trend in the atmospheric heat source over the Tibetan Plateau during recent decades. Part I: Observations. *J. Climate,* **21,** 3149–3164.

——, and ——, 2009: Weakening trend in the atmospheric heat source over the Tibetan Plateau during recent decades. Part II: Connection with climate warming. *J. Climate,* **22,** 4197–4212.

——, Y. Liu, and G. Wu, 2005: Heating status of the Tibetan Plateau from April to June and rainfall and atmospheric circulation anomaly over East Asia in midsummer. *Sci. China,* **48D,** 250–57.

——, G. Wu, Q. Zhang, and Y. Liu, 2006: New proofs of the recent climate warming over the Tibetan Plateau as a result of the increasing greenhouse gases emissions. *Chin. Sci. Bull.,* **51,** 1396–1400.

Flohn, H., 1960: Recent investigation on the mechanism of the ''summer monsoon'' of southern and eastern Asia. *Symposium on Monsoons of the World,* Hindu Union Press, 75–88.

Gong, D.-Y., and C.-H. Ho, 2002: Shift in the summer rainfall over the Yangtze River valley in the late 1970s. *Geophys. Res. Lett.,* **29,** 1436, doi:10.1029/2001GL014523.

Guo, Q. Y., 1983: The summer monsoon intensity index in East Asia and its variation (in Chinese). *Acta Geogr. Sin.,* **38,** 207–217.

Hahn, D. G., and S. Manabe, 1975: The role of mountains in the South Asian monsoon circulation. *J. Atmos. Sci.,* **32,** 1515–1541.

Holton, J. R., 1992: *An Introduction to Dynamic Meteorology*. International Geophysics Series, Vol. 48, Academic Press, 511 pp.

Hu, Z. Z., 1997: Interdecadal variability of summer climate over East Asia and its association with 500-hPa height and global sea surface temperature. *J. Geophys. Res.,* **102,** 19 403–19 412.

Huang, R. H., R. S. Cai, J. L. Chen, and L. T. Zhou, 2006: Interdecadal variations of drought and flooding disasters in China and their association with the East Asian climate system. *Chin. J. Atmos. Sci.,* **30,** 730–743.

Kalnay, E., and Coauthors, 1996: The NCEP/NCAR 40-Year Reanalysis Project. *Bull. Amer. Meteor. Soc.,* **77,** 433–471.

Kanamitsu, M., W. Ebisuzaki, J. Woollen, S.-K. Yang, J. J. Hnilo, M. Fiorino, and G. L. Potter, 2002: NCEP–DOE AMIP-II Reanalysis (R-2). *Bull. Amer. Meteor. Soc.,* **83,** 1631–1643.

Kwon, M., J.-G. Jhun, and K.-J. Ha, 2007: Decadal change in East Asian summer monsoon circulation in the mid-1990s. *Geophys. Res. Lett.,* **34,** L21706, doi:10.1029/2007GL031977.

Lau, K.-M., K.-M. Kim, and S. Yang, 2000: Dynamical and boundary forcing characteristics of regional components of the Asian summer monsoon. *J. Climate,* **13,** 2461–2482.

Li, G., T. Duan, J. Wan, Y. Gong, S. Haginoya, L. Chen, and W. Li, 1996: Determination of the drag coefficient over the Tibetan Plateau. *Adv. Atmos. Sci.,* **13,** 511–518.

——, ——, and Y. Gong, 2000: The bulk transfer coefficients and surface fluxes on the western Tibetan Plateau. *Chin. Sci. Bull.,* **45,** 1221–1226.

Li, J., and Q. Zeng, 2002: A unified monsoon index. *Geophys. Res. Lett.,* **29,** 1274, doi:10.1029/2001GL013874.

Liu, X., and B. Chen, 2000: Climatic warming in the Tibetan Plateau during recent decades. *Int. J. Climatol.,* **20,** 1729–1742.

Niu, T., L. X. Chen, and Z. J. Zhou, 2004: The characteristics of climate change over the Tibetan Plateau in the last 40 years and the detection of climatic jumps. *Adv. Atmos. Sci.,* **21,** 193–203.

Onogi, K., and Coauthors, 2007: The JRA-25 Reanalysis. *J. Meteor. Soc. Japan,* **85,** 369–432.

Rudolf, B., 2005: Global precipitation analysis products of the GPCC. Climate status report 2004, DWD Rep. Klimastatusbericht 2004, 163–170. [Available online at http://www.dwd.de/bvbw/generator/DWDWWW/Content/Oeffentlichkeit/KU/KU4/KU42/en/Reports__Publications/Analysis__Products__GPCC__KSB__2004__pdf,templateId=raw,property=publicationFile.pdf/Analysis_Products_GPCC_KSB_2004_pdf.pdf.]

Solomon, S., D. Qin, M. Manning, M. Marquis, K. Averyt, M. M. B. Tignor, H. L. Miller Jr., and Z. Chen, Eds., 2007: *Climate Change 2007: The Physical Science Basis*. Cambridge University Press, 996 pp.

Tao, S.-Y., and L.-X. Chen, 1987: A review of recent research on the East Asian summer monsoon in China. *Monsoon Meteorology,* C.-P. Chang and T. N. Krishnamurti, Eds., Oxford Monographs on Geology and Geophysics, Vol. 7, Oxford University Press, 60–92.

Wang, B., and Z. Fan, 1999: Choice of South Asian summer monsoon indices. *Bull. Amer. Meteor. Soc.,* **80,** 629–638.

Wang, Q., P. W. Guo, and Y. Y. Cao, 2007: Interdecadal variations of the relationship of spring thermal anomaly over eastern Tibetan Plateau and East Asian summer monsoon (in Chinese). *J. Nanjing Inst. Meteor.,* **30,** 259–265.

Wu, G., and Y. Zhang, 1998: Tibetan Plateau forcing and the timing of the monsoon onset over South Asia and the South China Sea. *Mon. Wea. Rev.,* **126,** 913–927.

——, W. Li, H. Guo, H. Liu, J. Xue, and Z. Wang, 1997: Sensible heat driven air-pump over the Tibetan Plateau and its impacts on the Asian summer monsoon. *Collections on the Memory of Zhao Jiuzhang* (in Chinese), Y. Duzheng, Ed., Chinese Science Press, 116–126.

——, and Coauthors, 2007: The influence of mechanical and thermal forcing by the Tibetan Plateau on Asian climate. *J. Hydrometeor.,* **8,** 770–789.

Yanai, M., C. Li, and Z. Song, 1992: Seasonal heating of the Tibetan Plateau and its effects on the evolution of the Asian summer monsoon. *J. Meteor. Soc. Japan,* **70,** 319–351.

Yeh, T. C., and Y. X. Gao, 1979: *Meteorology of the Qinghai-Xizang (Tibet) Plateau* (in Chinese). Chinese Science Press, 278 pp.

——, S. W. Lo, and P. C. Chu, 1957: On the heat balance and circulation structure in troposphere over Tibetan Plateau (in Chinese). *Acta Meteor. Sin.,* **28,** 108–121.

Zhang, Y. S., T. Li, and B. Wang, 2004: Decadal change of the spring snow depth over the Tibetan Plateau: The associated circulation and influence on the East Asian summer monsoon. *J. Climate,* **17,** 2780–2793.

Zhao, P., and L. X. Chen, 2001: Climate features of atmospheric heat source/sink over the Qinghai-Xizang Plateau in 35 years and its relation to rainfall in China. *Sci. China,* **44D,** 858–864.

Zhou, T. J., D. Y. Gong, J. Li, and B. Li, 2009: Detecting and understanding the multi-decadal variability of the East Asian summer monsoon: Recent progress and state of affairs. *Meteor. Z.,* **18,** 455–467.

Zhu, W., L. Chen, and X. Zhou, 2001: Several characteristics of contemporary climate change in the Tibetan Plateau. *Sci. China,* **44D** (Suppl.), 410–420.

Zhu, Y. X., Y. H. Ding, and H. D. Xu, 2007: The decadal relationship between atmospheric heat source of winter and spring snow over the Tibetan Plateau and rainfall in east China (in Chinese). *Acta Meteor. Sin.,* **65,** 946–958.